# Linking Notch signaling to ischemic stroke

**Joseph F. Arboleda-Velasquez*, Zhipeng Zhou†, Hwa Kyoung Shin†, Angeliki Louvi‡, Hyung-Hwan Kim§, Sean I. Savitz†, James K. Liao§, Salvatore Salomone†, Cenk Ayata†, Michael A. Moskowitz†, and Spyros Artavanis-Tsakonas*¶‖**

*Department of Cell Biology, Harvard Medical School, Boston, MA 02115; †Stroke and Neurovascular Regulation Laboratory, Massachusetts General Hospital, Boston, MA 02129; ‡Program on Neurogenetics and Department of Neurosurgery, Yale University School of Medicine, New Haven, CT 06520; §Vascular Medicine Research Unit, Brigham and Women's Hospital, Harvard Medical School, Cambridge, MA 02139; and ¶Collège de France, 75231 Paris, France

Edited by Pietro V. De Camilli, Yale University School of Medicine, New Haven, CT, and approved January 15, 2008 (received for review October 16, 2007)

**Vascular smooth muscle cells (SMCs) have been implicated in the pathophysiology of stroke, the third most common cause of death and the leading cause of long-term neurological disability in the world. However, there is little insight into the underlying cellular pathways that link SMC function to brain ischemia susceptibility. Using a hitherto uncharacterized knockout mouse model of *Notch 3*, a Notch signaling receptor paralogue highly expressed in vascular SMCs, we uncover a striking susceptibility to ischemic stroke upon challenge. Cellular and molecular analyses of vascular SMCs derived from these animals associate Notch 3 activity to the expression of specific gene targets, whereas genetic rescue experiments unambiguously link Notch 3 function in vessels to the ischemic phenotype.**

ischemia | Notch3 | vascular smooth muscle | CADASIL

Notch signaling defines one of the fundamental cell interaction mechanisms governing cell fate choices in metazoans (1, 2). The central element of this signaling pathway is the Notch cell surface receptor, a single-pass transmembrane protein, which interacts with membrane-bound ligands expressed on adjacent cells linking the fate of one cell to that of its neighbor (3, 4). In mammals, four paralogs of the Notch receptor have been identified, Notch 1–4, with overlapping but nonidentical expression patterns (5). In adult tissues, Notch 3 expression is restricted to vascular smooth muscle cells (SMCs) (5). Notwithstanding subtle arterial abnormalities reported in *Notch 3* mutant mice (6), the role of Notch 3 in vascular physiology remains unclear.

## Results

To explore Notch 3 function, we used a previously uncharacterized *Notch 3* knockout mouse model provided by W. C. Skarnes and M. Tessier-Lavigne (7). Like *Notch 3* knockouts studied in refs. 8 and 9, this mutant mouse was viable and fertile. The null allele was generated by insertional mutagenesis with a *lacZ* carrying vector so that $\beta$-galactosidase ($\beta$-gal) expression parallels that of *Notch 3* (Fig. 1). Our analysis generally agrees with reported *Notch 3* expression studies in the vasculature (10) but did reveal a broader distribution, including the neuronal progenitor-containing ventricular zone of the developing neural tube between embryonic day 12.5 (E12.5) and E15.5 and the neonatal brain [supporting information (SI) *Appendix*, SI Fig. 6, and data not shown]. Relevant to this study, *in situ* hybridization, X-gal staining, and immunofluorescence confirmed expression of Notch 3 in SMCs from brain vessels and aorta (Fig. 1 *D–F* and data not shown). A morphological study involving immunostaining with SMC-specific antibodies and electron microscopy did not reveal any abnormalities in either brain vessels or the aorta of knockout mice (Fig. 1*G*; *SI Appendix*, SI Fig. 7; and data not shown).

To investigate further the properties of SMCs lacking Notch 3 function, we developed a FACS-based cell purification protocol, taking advantage of the $\beta$-gal expression associated with the *Notch 3* knockout allele in SMCs, virtually the only cells in the adult brain to express Notch 3 (Figs. 1 and 2). Brain-derived cells from *Notch 3*$^{+/-}$ or *Notch 3*$^{-/-}$ mice were isolated and shown to express $\beta$-gal and specific markers confirming SMC identity (Fig. 2 *B* and *C* and *SI Appendix*, SI Fig. 8). Availability of a highly enriched population of SMCs allowed us to examine the impact of Notch 3 loss-of-function on the transcriptional profile of brain-derived SMCs (BrSMCs). Comparative analysis between Notch 3$^{+/-}$ and Notch 3$^{-/-}$ cells revealed 662 differentially regulated genes, using an arbitrary cutoff ($P \leq 0.01$, fold change $\pm$ 1.5). *Notch 3* scores as the utmost down-regulated gene (−22.1-fold) in Notch 3$^{-/-}$ BrSMCs. Indicative of their abnormal Notch signaling capacity, the canonical Notch downstream targets *Heyl* and *Hes1* were down-regulated (both −1.5-fold). Gene ontology analysis of all misregulated targets in BrSMCs showed statistical overrepresentation of genes classified under four functional categories named "muscle contraction" (all down-regulated), "cell structure and motility," "muscle development," and "mesoderm development" (*SI Appendix*, SI Tables 1 and 2), consistent with the notion that SMCs from knockout animals harbor significant functional differences compared with those carrying WT Notch 3 receptors.

Given the relevance of vascular SMCs to stroke, we examined the ischemia susceptibility of mice lacking Notch 3 function in a standard filament model of proximal middle cerebral artery (MCA) occlusion (11). In this assay, *Notch 3*$^{-/-}$ mice developed ischemic lesions approximately twice as large as those seen in WT or heterozygous (*Notch 3*$^{+/-}$) 10- to 12-week-old male mice (Fig. 3 *A* and *B*). Consistent with the severity of stroke, neurological deficits were more pronounced (Bederson neurological score on day 1 median values: WT = 1, *Notch 3*$^{-/-}$ = 2, $P < 0.01$) and mortality higher upon MCA occlusion in *Notch 3*$^{-/-}$ mice compared with WT (Fig. 3*C*). To assess whether enlarged infarcts were the result of more severe cerebral blood flow (CBF) deficits, we used laser speckle flowmetry (LSF) during distal MCA occlusion (12). This two-dimensional optical imaging technique measures cortical blood flow with high spatial resolution, quantifies the ischemic area, and allows for monitoring of spontaneous periinfarct depolarizations (PIDs) triggered by anoxic release of $K^+$ and excitatory amino acids from the infarct core (13, 14). Using this method, we found that *Notch 3*$^{-/-}$ mice developed a 60% larger area of severe CBF deficit than WT mice ($P < 0.01$) (Fig. 3 *D* and *E*). Thus, using two distinct approaches, we find complete loss of Notch 3 function to be associated with significant ischemic abnormalities. Interestingly, the frequency of spontaneous PIDs, which are known to aggravate stroke (15),

Author contributions: J.F.A.-V. and Z.Z. contributed equally to this work; J.F.A.-V., Z.Z., A.L., S.S., C.A., M.A.M., and S.A.-T. designed research; J.F.A.-V., Z.Z., H.K.S., A.L., H.-H.K., S.I.S., S.S., and C.A. performed research; J.F.A.-V., Z.Z., H.K.S., A.L., H.-H.K., S.I.S., J.K.L., S.S., C.A., M.A.M., and S.A.-T. analyzed data; and J.F.A.-V., A.L., C.A., M.A.M., and S.A.-T. wrote the paper.

The authors declare no conflict of interest.

This article is a PNAS Direct Submission.

‖To whom correspondence should be addressed. E-mail: artavanis@hms.harvard.edu.

This article contains supporting information online at www.pnas.org/cgi/content/full/0709867105/DC1.

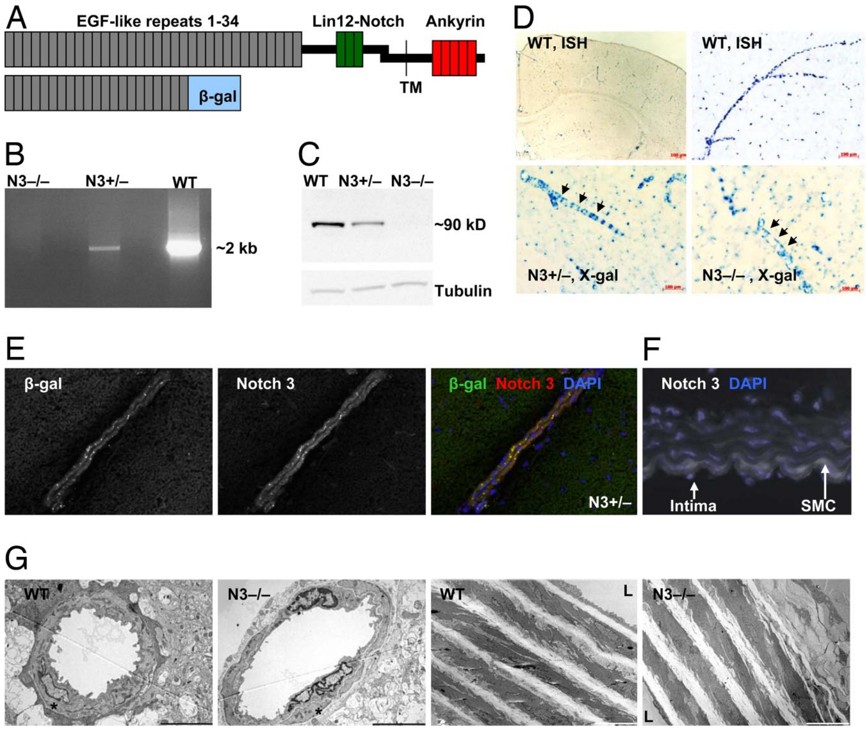


**Fig. 1.** Characterization of the *Notch 3* knockout mice. (*A*) A schematic of the heterodimeric Notch 3 receptor (*Upper*) indicating key structural features. In the extracellular domain, the 34 EGF-like repeats (gray boxes) and the three Lin12-Notch repeats (green boxes) are indicated. The transmembrane domain (TM), and the intracellular ankyrin repeat region are also shown (red boxes). The insertional mutagenesis, which generated the knockout allele, resulted in a fusion protein (*Lower*) containing EGF-like repeats 1–21 of Notch 3 fused to β-gal (blue box). (*B*) Long-range PCR amplified intron 16–17 (≈2 kb) of the *Notch 3* gene in DNA samples from WT (*Notch* $3^{+/+}$) or heterozygous animals (*Notch* $3^{+/-}$) but failed to amplify the larger intron containing the trapped vector in DNA from knockout mice (*Notch* $3^{-/-}$). (*C*) The Notch 3 intracellular domain was detected by Western blot analysis of cultured aortic smooth muscle cells (SMCs) derived from WT and *Notch* $3^{+/-}$ but absent (also by qRT-PCR, data not shown) in those derived from *Notch* $3^{-/-}$ mice. (*D*) Notch 3 expression. *In situ* hybridization, using a *Notch 3* antisense riboprobe labeled vessels in brain from WT mice (*Upper*). Likewise, X-gal staining (*Lower*) of *Notch* $3^{+/-}$ (*Left*) and *Notch* $3^{-/-}$ (*Right*) brain vessels. (*E*) Immunofluorescence of brain tissue sections demonstrated the colocalization of β-gal and Notch 3 extracellular epitopes in brain arteries from *Notch* $3^{+/-}$ mice. (*F*) Aortic SMC layers from WT mice (white) showed Notch 3 expression. (*G*) Low magnification electron micrographs of arterial cortical vessels (*Left*) and aorta (*Right*) from 8-week-old WT and *Notch* $3^{-/-}$ mice. Asterisks indicate smooth muscle cells. L, lumen. (Scale bars: *Left*, 5 μm; *Right*, 10 μm.)

was more than doubled in *Notch* $3^{-/-}$ compared with WT mice (6.0 ± 2.5 vs. 2.9 ± 2.5 PIDs per h, $P < 0.05$) (Fig. 4). However, *Notch* $3^{-/-}$ mice did not exhibit the characteristic transient hypoperfusion episodes during PIDs, suggesting that the vasoconstrictive ability of cerebral vessels was impaired in the mutants, an observation congruent with the down-regulation of muscle contraction genes unveiled by microarray analysis (Fig. 4). Systemic physiological variables (*SI Appendix*, SI Table 3) and absolute resting CBF (134 ± 45 ml·100 $g^{-1}$·$min^{-1}$ in *Notch* $3^{-/-}$, 136 ± 29 ml·100 $g^{-1}$·$min^{-1}$ in WT) and circle of Willis anatomy, examined by carbon black perfusion for the presence of communicating arteries (*SI Appendix*, SI Fig. 9), did not reveal any differences between WT and *Notch* $3^{-/-}$ mice that would explain the ischemic susceptibility.

To link unambiguously the ischemic phenotype with Notch 3 function, we deemed it essential to examine whether expression of WT Notch 3 in the SMCs could rescue the *Notch* $3^{-/-}$ ischemic phenotype. To that end, we generated a conditional transgenic mouse, ROSA *NOTCH 3*, which, when crossed to an appropriate Cre line [SM22-Cre (16)] could sustain SMC-specific expression of a human *NOTCH 3* transgene (Fig. 5). We found that expression of WT NOTCH 3 in vascular SMCs of knockout mice reduced infarct volume after filament occlusion of MCA (Fig. 5 *E* and *F*). Thus, Notch 3 expression in SMCs is both necessary and sufficient to rescue stroke susceptibility in knockout mice, directly linking the ischemic phenotype with Notch 3 function in SMCs.

## Discussion

Stroke burden is a key factor in determining short- and long-term neurological disability. Although not completely understood, extensive studies indicate that stroke burden varies greatly depending on complex interactions between blood vessels and brain cells (17). Here, we clearly link Notch signaling to ischemic stroke and raise the possibility that Notch 3 defines a key determinant of stroke burden through regulation of vascular SMC function.

Extensive functional studies of contractile activity in isolated aortas did not reveal differences between *Notch 3* knockout and WT animals (*SI Appendix*, SI Fig. 10). In contrast, abnormalities in contractile tone in cerebral vessels are suggested by the lack of vasoconstrictive response to PIDs during ischemia in *Notch* $3^{-/-}$ animals. Consistent with these data, the microarray analysis links *Notch 3* expression in SMCs from cerebral arteries with genes involved in vascular tone (*SI Appendix*, SI Tables 1 and 2), whereas no such link could be established when SMCs from aortas were used (data not shown). Whether the differences between brain and aorta SMCs revealed by these studies reflect genuine molecular phenotypic characteristics and distinct physiological properties remains to be determined.

The relevance of this study to human stroke is exemplified by the fact that *NOTCH 3* mutations, of obscure functional nature, are the only known cause of cerebral autosomal dominant arteriopathy with subcortical infarcts and leukoencephalopathy (CADASIL), a paradigmatic neurological disease characterized by vascular SMC pathology, progressive brain ischemia, and

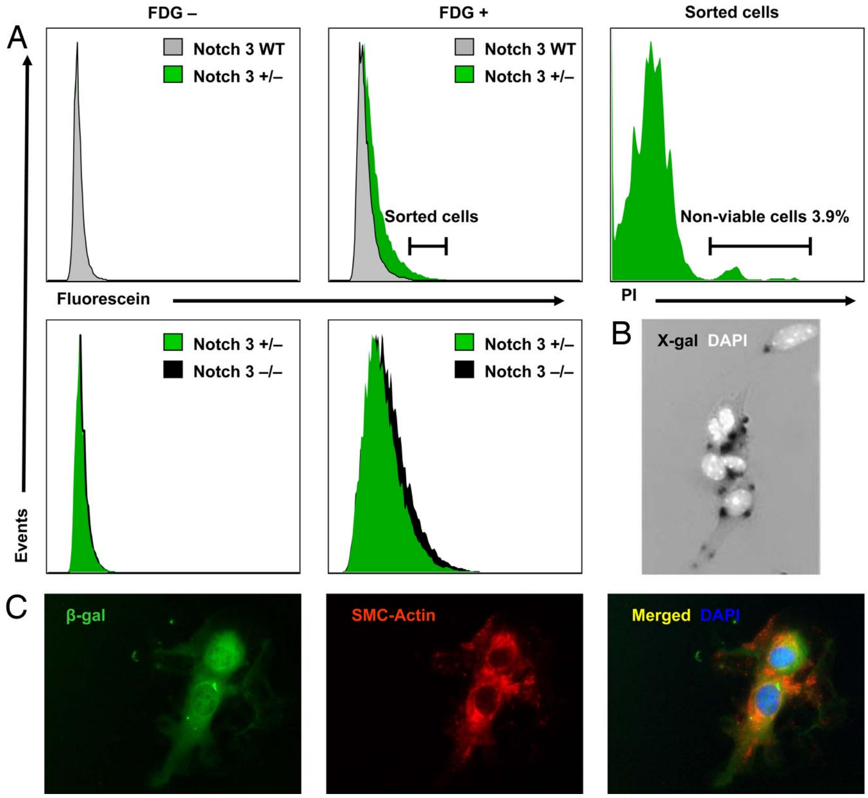


**Fig. 2.** Isolation of vascular smooth muscle cells from brain. (*A*) FACS analysis detected significant fluorescein-positive events in brain-derived cell suspensions from *Notch 3*$^{+/-}$ (β-gal positive) but not from WT mice (β-gal negative) upon incubation with the fluorogenic β-gal substrate fluorescein di-β-D-galactopyranoside (FDG) (*Center*). Most fluorescein-positive cells (96.1%) were viable as demonstrated by propidium iodide (PI) exclusion but were heterogeneously distributed in the FSC-A vs. SSC-A profile (*Right* and data not shown). In 20 independent FACS analyses performed by using our brain digestion and FDG staining protocols (including Notch 3$^{+/-}$ and Notch 3$^{-/-}$ samples), the percentage of PI-positive events in the total population ranged from 0.3 to 1.5%. Fluorescein signal was only occasionally higher in brain cell suspensions derived from *Notch* 3$^{-/-}$ mice (two copies of β-gal) compared with that of *Notch 3*$^{+/-}$ (one copy) (*Lower*) consistent with a documented nonlinear relationship between fluorescence intensity and intracellular β-galactosidase activity. (*B*) Seventy to 80% of fluorescein-positive sorted cells in culture showed X-gal staining. (*C*) β-gal positive cells always expressed smooth muscle-specific alpha actin epitopes (SMC-actin).

vascular cognitive impairment (18, 19). Although vascular abnormalities in CADASIL are widespread, anatomical studies have shown a predilection of *NOTCH 3*-associated pathology for small vessels particularly in those brain regions with lowest blood flow values, such as the white matter (20).

The availability of appropriate mouse models to study the role of Notch 3 in brain ischemia is of significance because CADASIL is a prevalent cause of stroke and vascular cognitive impairment in humans and because such models may prove valuable in increasing our general understanding of the cellular and molecular mechanisms underlying stroke pathophysiology.

## Materials and Methods

**Animal Protocols.** Animal care and experimental procedures were performed with approval from institutional animal care and use committees of Massachusetts General Hospital, Harvard Medical School and Yale University. Littermates were used for comparative analysis throughout.

***In Situ* Hybridization and Detection of β-Galactosidase Activity.** Animals were fixed by transcardiac perfusion with 4% paraformaldehyde in PBS. Brains were removed, fixed overnight in 30% sucrose and 4% paraformaldehyde, and sectioned in the coronal plane on a sledge cryomicrotome (Leica SM2000) at 40 μm. *In situ* hybridization was essentially performed as described in refs. 21 and 22. X-gal staining was performed overnight at 30°C in a solution containing 0.5 mM potassium ferricyanide, 0.5 mM potassium ferrocyanide, 20 mM $MgCl_2$, 0.1% Triton X-100, and 0.37 mg/ml X-gal.

**Purification of Brain-Derived SMCs.** Ten- to 12-week-old male mice were killed and perfused with 10 ml of PBS before brain dissection. After removal of the meninges, brain tissues were fragmented with a razor blade and digested in 10 ml of PBS (without calcium or magnesium) supplemented with a collagenase/dispase mixture (100 μg/ml, Roche), incubated for 75 min at 37°C, and homogenized by using a 10-ml pipette. Undigested material was removed by using a 100-μm cell strainer. The flow-through was centrifuged at 4°C for 3 min at 834 × *g* and the pellet washed with 10 ml of PBS (with calcium and magnesium) four times. Cells were resuspended in Opti-MEM (without phenol red; Invitrogen) before staining with fluorescein di-β-D-galactopyranoside (FDG), a fluorogenic substrate for β-gal (Fluka), using standard methodology (23) modified as follows: FDG stock was prepared in a $H_2O$:Ethyl:DMSO (8:1:1) solution to a final concentration of 30 mM and kept frozen at −20°C. For staining, 2 mM FDG (in 100 μl of $H_2O$) and cells (in 100 μl of medium; $1 \times 10^7$ cells per ml) were preincubated for 5 min at 37°C, mixed together, and then incubated for 1 min at 37°C to induce FDG uptake. The reaction was stopped by adding 0.8 ml of Opti-MEM and incubation on ice. Individual cell preparations were finally pooled, centrifuged 3 min, and resuspended in Opti-MEM (at concentrations 2–10 × $10^6$ cells per ml) before FACS analysis and sorting. In β-gal positive cells, FDG is metabolized to fluorescein allowing FACS sorting and culture of brain-derived SMCs. This method typically yields $7.5 \times 10^4$ to $1 \times 10^5$ fluorescein-positive cells per adult mouse brain. These were routinely kept for 1–7 days in culture (F12/MEM and 10% FBS; Invitrogen) or fixed with 4% paraformaldehyde before immunofluorescence studies. Purity of the SMC preparations was determined by using X-gal staining, and antibodies specific for Notch 3 and α-smooth muscle actin (see *SI Appendix*), thus they may also contain pericytes.

**Microarray Studies.** Biotinylated cRNA samples from freshly sorted brain SMCs (four *Notch 3*$^{+/-}$ mice and five *Notch 3*$^{-/-}$ mice) were fragmented before hybridization (15 μg each) onto mouse 430 2.0 Affymetrix chips. The chips were washed, stained by using strepavidin-phycoerytrin, and scanned the next

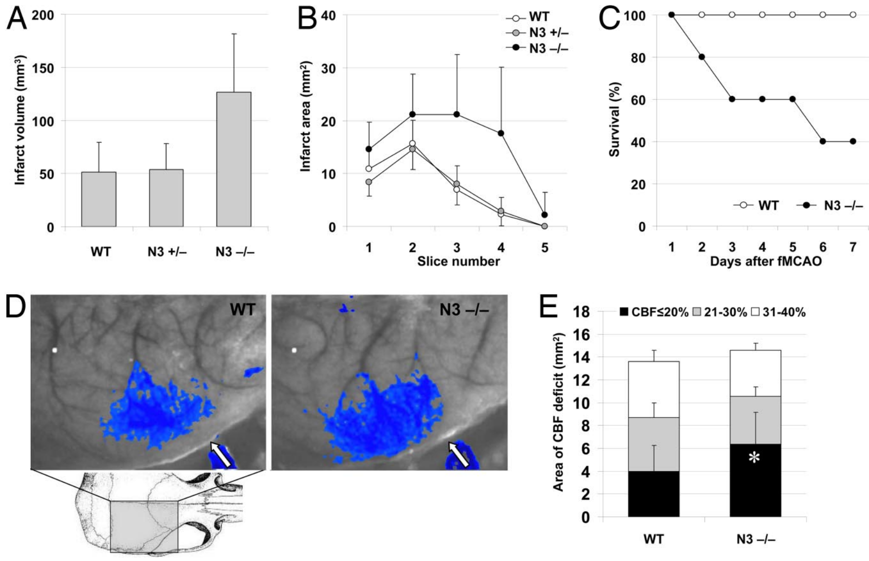


**Fig. 3.** Stroke susceptibility of *Notch 3* knockout mice. (*A* and *B*) Infarct volume (indirect method) and infarct areas in individual coronal slices in WT, *Notch 3*$^{+/-}$ (N3$^{+/-}$), and *Notch 3*$^{-/-}$ (N3$^{-/-}$) mice analyzed 22 h after a 1-h transient filament middle cerebral artery occlusion (fMCAO). Both infarct area and volume were substantially larger in *Notch 3*$^{-/-}$ mice compared with those of WT and *Notch 3*$^{+/-}$ mice (10- to 12-week-old male mice, $n = 9$ per group; $P < 0.01$). (*C*) A separate cohort of WT and *Notch 3*$^{-/-}$ mice (10- to 12-week-old male mice, $n = 5$ per group) underwent 1 h transient fMCAO. *Notch 3*$^{-/-}$ mice had 60% mortality over 7 days, compared with no mortality in WT mice. (*D*) Representative laser speckle contrast images taken 1 h after distal MCA occlusion (dMCAO) are shown from WT and *Notch 3*$^{-/-}$ mice. Distal MCA was clipped through a small temporal craniotomy (arrows). Superimposed areas (blue) indicate regions with severe cerebral blood flow (CBF) deficit (i.e., <20% residual CBF). *Notch 3*$^{-/-}$ mice developed significantly larger area of severe CBF deficit compared with WT. The imaging field (5.24 × 7 mm) was positioned over the entire right hemisphere as shown in *Left Inset*. (*E*) Composite bar graph showing the areas of severe (residual CBF ≤20%), moderate (21–30%), and mild (31–40%) CBF deficit in WT and *Notch 3*$^{-/-}$ mice 60 min after dMCAO. The area of severe CBF deficit was significantly larger in *Notch 3*$^{-/-}$ animals compared with WT ($P < 0.01$), whereas the areas of moderate or mild CBF deficit did not differ between the two genotypes ($P > 0.05$; two way ANOVA for repeated measures). Error bars indicate standard deviations.

day as described in ref. 24. For data normalization, all probe sets were scaled to a target intensity of 150. Microarray data analysis was performed by using Rosetta Resolver. All cells were from 10- to 12-week-old male mice.

**Gene Ontology Analyses.** PANTHER software was used to define over- and underrepresented functions in the list of signature genes found by microarray analysis (25). *P* values were calculated by using binomial statistics.

**Model of Focal Cerebral Ischemia.** Animals were anesthetized with 2% isoflurane and maintained on 1.5% isoflurane in 70% $N_2O$ and 30% $O_2$ by a face mask. Cerebral infarcts were produced by 1 h of MCA occlusion followed by reperfusion as described in refs. 11, 26, and 27. Regional CBF and physiologic parameters were monitored as described in refs. 11, 26, and 27. Infarct volumes were calculated by integrating the infarct area in each brain section of the brain, using the indirect method to correct for edema.

**Determination of Infarct Size.** After kill, cerebral infarct sizes were determined on 2,3,5-triphenyltetrazolium chloride (TTC, 22 h)-stained 2-mm brain sections by means of an image analysis system (M4; Imaging Research) as described in refs. 11, 26, and 27.

**Neurological Evaluation.** Mice that underwent 1 h of fMCAO were evaluated for neurological deficits over a period of 1 week. Deficits were measured on a well established five-point neurological scale (28): 0, no neurologic deficit; 1, failure to extend the left forepaw fully; 2, circling to the left; 3, falling or leaning over to the left; 4, no spontaneous walking and a depressed level of consciousness; or 5, dead. All animals tested had a score of 0 before undergoing fMCAO.

**Laser Speckle Flowmetry (LSF).** Adult mice were anesthetized with isoflurane (2% induction, 1% maintenance), endothracheally intubated, and ventilated. Blood pressure and heart rate were continuously recorded by using PowerLab (ADInstruments). Physiological monitoring (blood pressure, arterial blood gases, and pH) was performed at least once every hour, and the adequacy of anesthesia was regularly checked by the absence of a blood pressure response to tail pinch. After general surgical preparation, mice were placed in a stereotaxic frame, and skull surface was prepared for LSF to study the spatiotemporal characteristics of

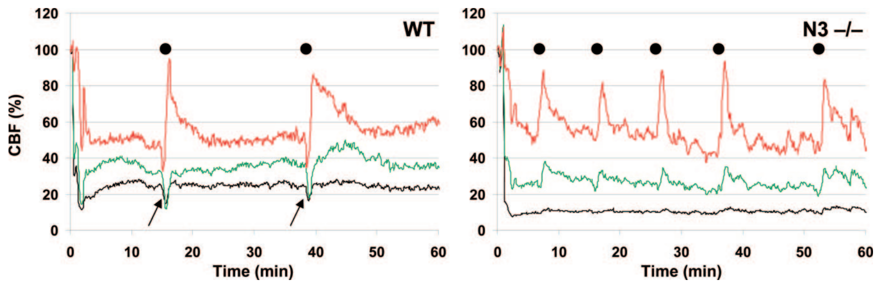


**Fig. 4.** Abnormal CBF changes upon ischemic challenge in *Notch 3* knockout mice. Representative tracings showing the time-course of CBF changes after dMCAO (at time 0) in severe (black), moderate (green), or mildly ischemic cortex (red) in WT and *Notch 3*$^{-/-}$ (N3$^{-/-}$) mice. Black dots indicate spontaneous peri-infarct depolarizations (PIDs). *Notch 3*$^{-/-}$ mice developed more frequent PIDs; however, the characteristic transient hypoperfusion response observed in WT during the PIDs (arrows) was absent in *Notch 3*$^{-/-}$ mice.

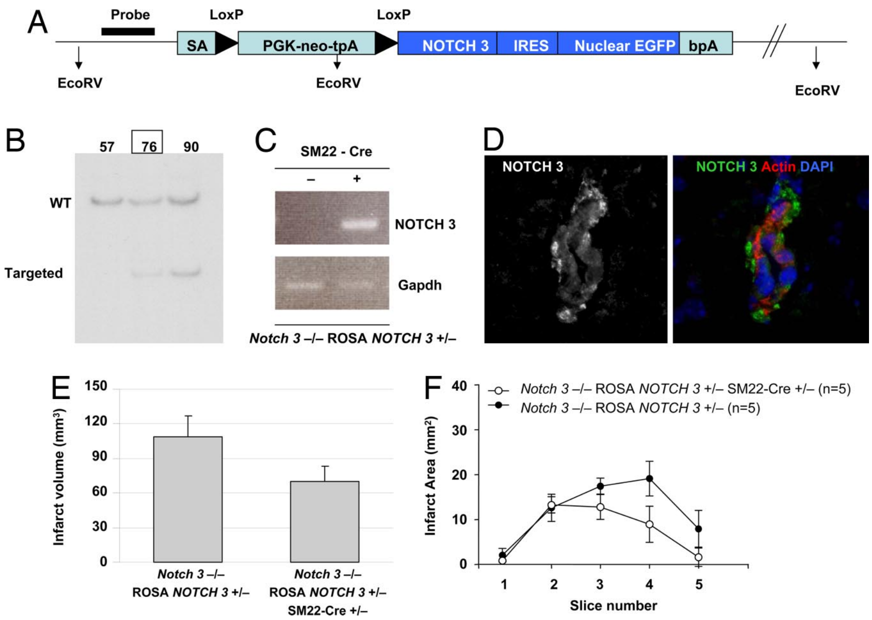


**Fig. 5.** Rescuing stroke susceptibility with human *NOTCH* 3. (*A*) Schematic representation of the targeting construct used to generate mice carrying a WT human *NOTCH* 3 transgene that can be conditionally expressed by Cre-mediated recombination. The vector contains ROSA genomic sequences allowing for homologous recombination in the ROSA locus, an adenovirus splice acceptor site (SA), a PGK-neo-tpA ''stop'' cassette flanked by LoxP sites (black triangles), the coding region for human *NOTCH 3*, an internal ribosomal entry sequence (IRES), nuclear EGFP, and the bovine growth hormone polyadenylation sequence (bpA). (*B*) The EcoRV restriction sites allowed identification of WT vs. targeted alleles by Southern blot analysis of DNA from ES cell clones (clone 76 generated chimeric mice capable of germ line transmission). (*C* and *D*) Upon Cre expression, the PGK-Neo-tpA cassette is excised, thereby allowing expression of the *NOTCH 3* transgene detected here by RT-PCR in aorta tissue (*C*) and in brain arterioles from a *Notch* $3^{-/-}$; ROSA *NOTCH* $3^{+/-}$; SM22-Cre$^{+/-}$ mouse (Cre under the control of the smooth muscle-specific transgelin promoter), using an antibody specific for intracellular epitopes of the receptor (*D*). (*E* and *F*) Graphics depict indirect infarct volume and infarct area of genetically rescued (*Notch* $3^{-/-}$; ROSA *NOTCH* $3^{+/-}$; SM22-Cre$^{+/-}$) and control (*Notch* $3^{-/-}$; ROSA *NOTCH* $3^{+/-}$) mice after 1 h of MCAO and 22 h of reperfusion (10- to 12-week-old male mice, $n = 5$ per group; $P < 0.01$). Error bars represent standard deviations.

cerebral blood flow (CBF) changes during focal ischemia. Focal ischemia was induced by clipping the MCA and LSF imaging was initiated 1 min before MCA ligation and continued up to 90 min. Images obtained by a CCD camera positioned above the head were analyzed by using three separate paradigms to determine the time course of CBF changes, the area of severe, moderate or mildly ischemic cortex, and the CBF profile between the nonischemic cortex and the ischemic core (12).

**Generation of ROSA *NOTCH 3* Mice.** We generated a conditional knockin mouse to determine tissue-specific requirements for Notch 3 expression. For this purpose, the human *NOTCH 3* cDNA generously provided to us by E. Tournier-Lasserve (Institut National de la Santé, et de la Recherche Médicale U740, Paris, France) was subcloned into a vector designed for site-specific recombination into the ubiquitously expressed ROSA26 mouse locus (29). In the final construct, *NOTCH 3* was flanked by a loxed stop cassette at the 5′end (for Cre-mediated regulation of expression) and an IRES-nuclearGFP sequence at the 3′ end. The resulting construct was sequenced and electroporated into ES cells (129SV/J line) before selection of positive clones by long-range PCR and Southern blot hybridization. Chimeras generated through embryo injections of ES cells clones were crossed to C57BL/6 mice to obtain germ-line transmission. The resulting ROSA *NOTCH 3* knockin mice (WT76 line) were viable and fertile and displayed no gross abnormalities.

**ACKNOWLEDGMENTS.** We thank Michael Waring and the Harvard Medical School Center for AIDS Research Immunology Core at Massachusetts General Hospital for help with cell sorting and optimization of the FDG-based purification methods; Charles Vanderburg, Rachel Diamond, and the Harvard Center for Neurodegeneration and Repair's Advanced Tissue Resource Center for RNA preparation and analysis; Christoph Rahner and the Center for Cell and Molecular Imaging at Yale University School of Medicine for help with electron microscopy; Katia Georgopoulos, Lin Wu, Jeffrey Wu, and the Massachusetts General Hospital transgenic mouse core facility for assistance in the generation of knockin mice lines; Kathryn Coser and the Massachusetts General Hospital Cancer Center DNA Microarray Core; and Emily McKillip, David Wilson, and Seo-Kyoung Hwang for technical assistance. This work was supported by National Institutes of Health Grants to S.A.-T. (HG003616-01A1, CA098402-06, and NS026084-18), J.K.L. (HL052233), and M.A.M. (5 P50 NS10828-32) and by Yale University School of Medicine (A.L.).

1. Hurlbut GD, Kankel MW, Lake RJ, Artavanis-Tsakonas S (2007) Crossing paths with Notch in the hyper-network. *Curr Opin Cell Biol* 19:166–175.
2. Louvi A, Artavanis-Tsakonas S (2006) Notch signalling in vertebrate neural development. *Nat Rev Neurosci* 7:93–102.
3. Artavanis-Tsakonas S, Rand MD, Lake RJ (1999) Notch signaling: Cell fate control and signal integration in development. *Science* 284:770–776.
4. Bray SJ (2006) Notch signalling: A simple pathway becomes complex. *Nat Rev Mol Cell Biol* 7:678–689.
5. Hofmann JJ, Iruela-Arispe ML (2007) Notch signaling in blood vessels: Who is talking to whom about what? *Circ Res* 100:1556–1568.
6. Domenga V, *et al.* (2004) Notch3 is required for arterial identity and maturation of vascular smooth muscle cells. *Genes Dev* 18:2730–2735.
7. Mitchell KJ, *et al.* (2001) Functional analysis of secreted and transmembrane proteins critical to mouse development. *Nat Genet* 28:241–249.
8. Krebs LT, *et al.* (2003) Characterization of Notch3-deficient mice: Normal embryonic development and absence of genetic interactions with a Notch1 mutation. *Genesis* 37:139–143.
9. Kitamoto T, *et al.* (2005) Functional redundancy of the Notch gene family during mouse embryogenesis: Analysis of Notch gene expression in Notch3-deficient mice. *Biochem Biophys Res Commun* 331:1154–1162.
10. Prakash N, Hansson E, Betsholtz C, Mitsiadis T, Lendahl U (2002) Mouse Notch 3 expression in the pre- and postnatal brain: Relationship to the stroke and dementia syndrome CADASIL. *Exp Cell Res* 278:31–44.
11. Huang Z, *et al.* (1994) Effects of cerebral ischemia in mice deficient in neuronal nitric oxide synthase. *Science* 265:1883–1885.
12. Ayata C, *et al.* (2004) Laser speckle flowmetry for the study of cerebrovascular physiology in normal and ischemic mouse cortex. *J Cereb Blood Flow Metab* 24:744–755.
13. Shin HK, *et al.* (2006) Vasoconstrictive neurovascular coupling during focal ischemic depolarizations. *J Cereb Blood Flow Metab* 26:1018–1030.
14. Hossmann KA (1996) Periinfarct depolarizations. *Cerebrovasc Brain Metab Rev* 8:195–208.
15. Selman WR, Lust WD, Pundik S, Zhou Y, Ratcheson RA (2004) Compromised metabolic recovery following spontaneous spreading depression in the penumbra. *Brain Res* 999:167–174.
16. Holtwick R, *et al.* (2002) Smooth muscle-selective deletion of guanylyl cyclase-A prevents the acute but not chronic effects of ANP on blood pressure. *Proc Natl Acad Sci USA* 99:7142–7147.
17. Lo EH, Dalkara T, Moskowitz MA (2003) Mechanisms, challenges and opportunities in stroke. *Nat Rev Neurosci* 4:399–415.

18. Joutel A, *et al.* (1996) Notch3 mutations in CADASIL, a hereditary adult-onset condition causing stroke and dementia. *Nature* 383:707–710.
19. Ruchoux MM, Maurage CA (1997) CADASIL: Cerebral autosomal dominant arteriopathy with subcortical infarcts and leukoencephalopathy. *J Neuropathol Exp Neurol* 56:947–964.
20. Louvi A, Arboleda-Velasquez JF, Artavanis-Tsakonas S (2006) CADASIL: A critical look at a Notch disease. *Dev Neurosci* 28:5–12.
21. Grove EA, Tole S, Limon J, Yip L, Ragsdale CW (1998) The hem of the embryonic cerebral cortex is defined by the expression of multiple Wnt genes and is compromised in Gli3-deficient mice. *Development* 125:2315–2325.
22. Tole S, Patterson PH (1995) Regionalization of the developing forebrain: A comparison of FORSE-1, Dlx-2, and BF-1. *J Neurosci* 15:970–980.
23. Nolan GP, Fiering S, Nicolas JF, Herzenberg LA (1988) Fluorescence-activated cell analysis and sorting of viable mammalian cells based on beta-D-galactosidase activity after transduction of *Escherichia coli* lacZ. *Proc Natl Acad Sci USA* 85:2603–2607.
24. Coser KR, *et al.* (2003) Global analysis of ligand sensitivity of estrogen inducible and suppressible genes in MCF7/BUS breast cancer cells by DNA microarray. *Proc Natl Acad Sci USA* 100:13994–13999.
25. Cho RJ, Campbell MJ (2000) Transcription, genomes, function. *Trends Genet* 16:409–415.
26. Huang Z, *et al.* (1996) Enlarged infarcts in endothelial nitric oxide synthase knockout mice are attenuated by nitro-L-arginine. *J Cereb Blood Flow Metab* 16:981–987.
27. Endres M, Wang ZQ, Namura S, Waeber C, Moskowitz MA (1997) Ischemic brain injury is mediated by the activation of poly(ADP-ribose)polymerase. *J Cereb Blood Flow Metab* 17:1143–1151.
28. Bederson JB, *et al.* (1986) Rat middle cerebral artery occlusion: evaluation of the model and development of a neurologic examination. *Stroke* 17:472–476.
29. Zambrowicz BP, *et al.* (1997) Disruption of overlapping transcripts in the ROSA beta geo 26 gene trap strain leads to widespread expression of beta-galactosidase in mouse embryos and hematopoietic cells. *Proc Natl Acad Sci USA* 94:3789–3794.